THE EUROPEAN SOCIETY OF MEDICINE
Medical Research Archives, Volume 13 Issue 8

RESEARCH ARTICLE

Dosimetry Characterization and Early-Phase Dose and Injury-Severity Biomarkers in a Rhesus Macaque Dose-Response Model System

Arifur Rahman [1,2#], David J. Sandgren [2], Vitaly Nagy [2], Sung-Yop Kim [2#], David L. Bolduc [2], and William F. Blakely [2*]

[1] Henry M Jackson Foundation, 6720A Rockledge Drive, Bethesda, MD USA;
[2] Armed Forces Radiobiology Research Institute, Uniformed Services University of the Health Sciences, 4555 South Palmer Road, Bethesda, MD 20889-5648 USA

*Corresponding author:
william.blakely@usuhs.edu
Voice: 301.295.0484
#Authors present addresses: (AR) Biology, Rockville campus, Montgomery College, 51 Mannakee Streeet, Rockville, MD 20850 USA; (S-YK) Walter Reed National Military Medical Center, Bethesda, 8960 Brown Dr., Bldg. 85T, 2nd Floor, Room 2C45, Bethesda, MD 20889-5629 USA

OPEN ACCESS

PUBLISHED
31 August 2025

CITATION
Rahman, A., Sandgren, DJ., et al., 2025. Dosimetry Characterization and Early-Phase Dose and Injury-Severity Biomarkers in a Rhesus Macaque Dose-Response Model System. Medical Research Archives, [online] 13(8).
https://doi.org/10.18103/mra.v13i8.6676

COPYRIGHT
© 2025 European Society of Medicine. This is an open-access article distributed under the terms of the Creative Commons Attribution License, which permits unrestricted use, distribution, and reproduction in any medium, provided the original author and source are credited.

DOI
https://doi.org/10.18103/mra.v13i8.6676

ISSN
2375-1924

ABSTRACT

The purpose of this study was to characterize radiation dosimetry and validate early-phase radiation biomarkers using a Rhesus macaque (*Macaca mulatta*) non-human-primate radiation model. Non-human-primates in pairs (male and females; 4.4 to 7.8 kg; 3.6 to 5.9 y) were exposed bilaterally to ^{60}Co-gamma rays to midline doses of 0, 1, 3.5, 6.5 and 8.5 Gy at ~0.55 Gy/min (n = 6/dose). The exposure intervals were determined based on dose-rate measurements using cylindrical water phantoms with the alanine – electron paramagnetic resonance system traceable to the National Institute of Standards and Technology. Field uniformity was characterized and the physics reference doses were measured at the mid-line at the height of the xiphoid process. Blood was sampled for measurements of hematology and blood chemistry radio-responses prior to irradiation and up to 4 d after exposure. The field in the area occupied by the animals was uniform within approximately ± 0.5% in the lateral direction, within approximately ± 1.5% in the anterior-posterior direction, and within approximately ± 2% in the superior-inferior direction. Exposure to 1, 3.5, 6.5, and 8.5 Gy causes a dramatic increase in amylase activity (~1.9, ~3.1, ~8.3, ~13.3 fold, respectively) at 1 d after exposure (p= <0.001) along with more than 60, 80, and 90% depletion of lymphocyte at 1, 3.5, and higher doses 6.5 or 8.5 Gy, respectively. Hematological (i.e., lymphocyte depletion and increases in neutrophil to lymphocyte ratios at 1-3 d) and blood chemistry (i.e., serum amylase activity at 1 d) radiation biomarkers demonstrate useful diagnostic utility for life-threatening radiation exposure assessment.

Keywords: biodosimetry, ^{60}Co-γ-rays, rhesus macaque, hematology, amylase activity, radiation dosimetry, alanine, electron paramagnetic resonance.

Introduction

First responders and receivers in the aftermath of a radiological terrorism incident or mass-casualty radiation accident require prior guidance and pre-positioned resources for assessment, triage, and medical management of affected individuals. Several articles [1-5] as well as national [6-8] and international [9] agencies have reviewed strategies for acute-phase biodosimetry. Consensus biodosimetric guidelines include: a) clinical signs and symptoms, including peripheral blood counts, time to onset of nausea and vomiting, and presence of impaired cognition and neurological deficits, b) radioactivity assessment, c) personal and area dosimetry, d) cytogenetics, e) *in vivo* electron paramagnetic resonance (EPR), and f) other dosimetry approaches (i.e. blood protein assays, etc.) [3,10]. Emerging biodosimetric technologies may further refine triage and dose assessment strategies. Guidance, however, is needed for currently available biodosimetry techniques that are most useful for different radiological scenarios and consensus protocols must be developed.

Hematological responses are early-response biomarkers for radiation dose assessment and also contribute in the measurement of the severity of hematopoietic-acute radiation syndrome (H-ARS). Fliedner and colleagues advocate the use of changes in blood cell (i.e., lymphocytes, granulocytes, and platelets) profiles after whole-body radiation exposures. Reliable haematological bioindicators of injury are critical aids to plan therapeutic treatments [11-12]. An approximate 50% decline in peripheral blood lymphocyte counts over 12 hours that drop below normal values (1.4 x 10^9/L) is indicative of a potential severe radiation overexposure [2]. Guskova and colleagues used lymphocyte cell counts measured 1-9 d post-radiation for dose assessment after acute photon equivalent radiation exposures [9]. Goans and colleagues introduced the use of lymphocyte depletion kinetic models for dose estimates based on human radiation-accident registry data for whole-body acute gamma exposures [13] and more recently for criticality accidents [14]. Azizova and colleagues, using haematology data from nuclear accident cases at Mayak Production Association [15], suggested that the ratio of neutrophils to lymphocytes may provide a useful early-phase biodosimeter.

Radiation is reported to cause elevations in serum amylase activity; see references cited in Blakely et al. [16-17]. Blakely and colleagues showed using a Rhesus macaque – radiation model significant changes in serum amylase activity 1d after total-body irradiation (TBI) to 6.5 Gy ^{60}Co-γ-rays, which return to normal by 6d [16]. Radiation induced elevations in serum amylase activity were confirmed in an additional Rhesus macaque radiation model involving 6.5 Gy exposure [17]. Furthermore, use of serum amylase activity and hematology (i.e., lymphocyte, neutrophils, and ratio of neutrophils to lymphocytes) resulted in 100% successful separation of exposed macaques (24 h after TBI) vs. samples from the same macaques taken before irradiation using discriminant analysis [17]. These results confirm that radiation produces acute changes in amylase activity and blood cell counts, useful in assessing radiation-induced injury and dose.

The need to rapidly assess radiation exposure and injury in mass-casualty and population-monitoring scenarios prompted a dose-response based evaluation of suitable biomarkers that can provide early-phase diagnostic information after exposures. Here we report the physical dosimetry characterization of a dose-response model and investigated the dose-dependency for the use of serum amylase activity and hematological blood-cell count biomarkers to provide early-phase assessment of severe radiation exposures in a non-human primate model (i.e., rhesus macaques; n=24). Our results demonstrate that early-phase changes in hematology (i.e., lymphocyte depletion and increases in neutrophil to lymphocyte ratios at 1-3d) and blood chemistry (i.e., serum amylase activity at 1d) radiation biomarkers demonstrate useful diagnostic utility for assessment of life-threatening radiation exposure dose and injury assessment.

Materials and Methods

2.1 RADIATION DOSIMETRY

2.1.1 Radiation Source and Setup for Exposure of Non-human Primates in Plexiglas® Boxes

The animals were irradiated bilaterally at the Armed Forces Radiobiology Research Institute (AFRRI) to whole-body radiation of ^{60}Co-gamma rays (1.0, 3.5, 6.5, and 8.5 Gy; n = 6 in each cohort) as well as sham controls (n = 6) using the Co-60 facility, which provided a highly uniformed radiation field with an adjustable dose rate as previously reported [18-19]. The ^{60}Co sources are positioned at both ends of a pool (i.e., tank of water) and raised out of the water for irradiations. Two Plexiglas® boxes, with one immobilized animal in each, were positioned on a table between two radiation sources so that the animals were oriented back-to-back with respect to each other (Fig. 1).

The radiation beams were directed perpendicularly to the table (along the Y axis) and, thus, penetrated the animals from side to side. Each of the two ^{60}Co sources consisted of 16 rods (l = 63.5 cm; D = 2.5 cm) containing pellets of radioactive metallic cobalt in stainless-steel shells. The rods of each source were arranged vertically in a plane parallel to the larger side of the exposure table (i.e., parallel to the XZ plane in Fig. 1), effectively providing a radioactive panel 63.5 × 63.5 cm^2. The heights of the centers of the panels approximately corresponded to the heights of the cores of abdomens of the primates. The distance from each of the sources to the middle of the table (axis X in the figures and mid planes of the animals) was 228 cm in all irradiations.

© 2025 European Society of Medicine

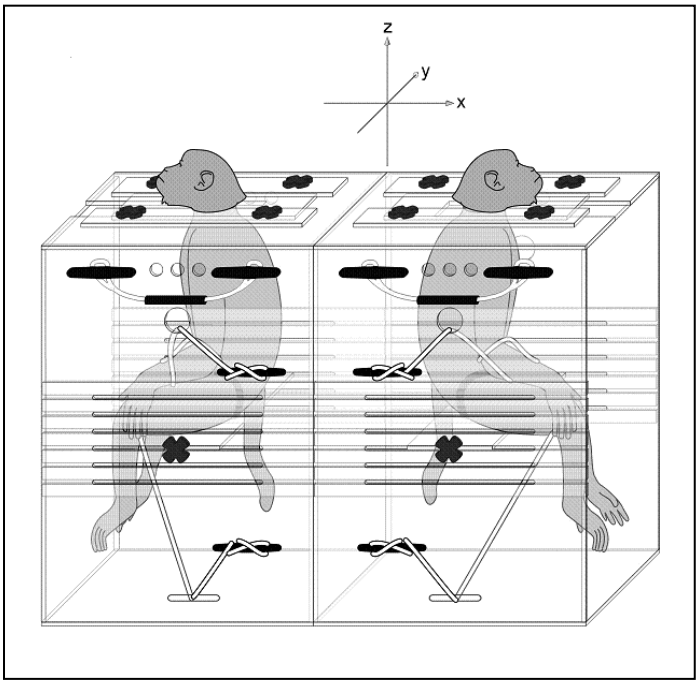

Fig. 1. Schematic representation of NHP's image in two Plexiglas® boxes. One immobilized animal in each box. Animals were oriented back-to-back with respect to each other. The radiation beams were directed perpendicularly to the table and, thus penetrated the animals from side to side.

2.1.2 Radiation Field Uniformity Measurement within the Plexiglas® Boxes

The uniformity data of the radiation field used for the irradiations of the animals were tested with Kodak V-Xomat V radiographic films. The exposed and developed films were scanned with a Vidar scanner (Vidar Systems Corp., Herndon, VA, USA), and the images were processed with the RIT software (Radiological Imaging Technology, Inc., Colorado Springs, CO, USA).

2.1.3 Dose Rate and Exposure-Time Determination

Very high stability of the dose rate of Co-60 beams during an irradiation session and its exact predictability on any given date made it possible to provide doses by specifying exposure times calculated from precisely measured dose rates. The dose rate was accurately measured before the start of this study, and the dose rate on each of the days of irradiation were calculated by applying the decay correction exactly known from the Co-60 half-life of 1925.23 d [20].

Radiation doses were measured using the alanine/EPR dosimetry technique [21-25]. Alanine pellets FWT-50-10 from Far West Technology, Inc. (Goleta, CA) and EPR spectrometer e-Scan (Bruker Biospin Corp., Germany) specifically designed for alanine dosimetry were used. As the phantoms were manufactured from Plexiglas® and filled with water, they were approximately tissue-equivalent from the view point of radiation physics of the ^{60}Co photons. Dosimetry, performed using an alanine/electron paramagnetic resonance system, was calibrated against the National Institute of Standards and Technology and further verified by an additional check against the national standard ^{60}Co source of UK National Physics Laboratory [22].

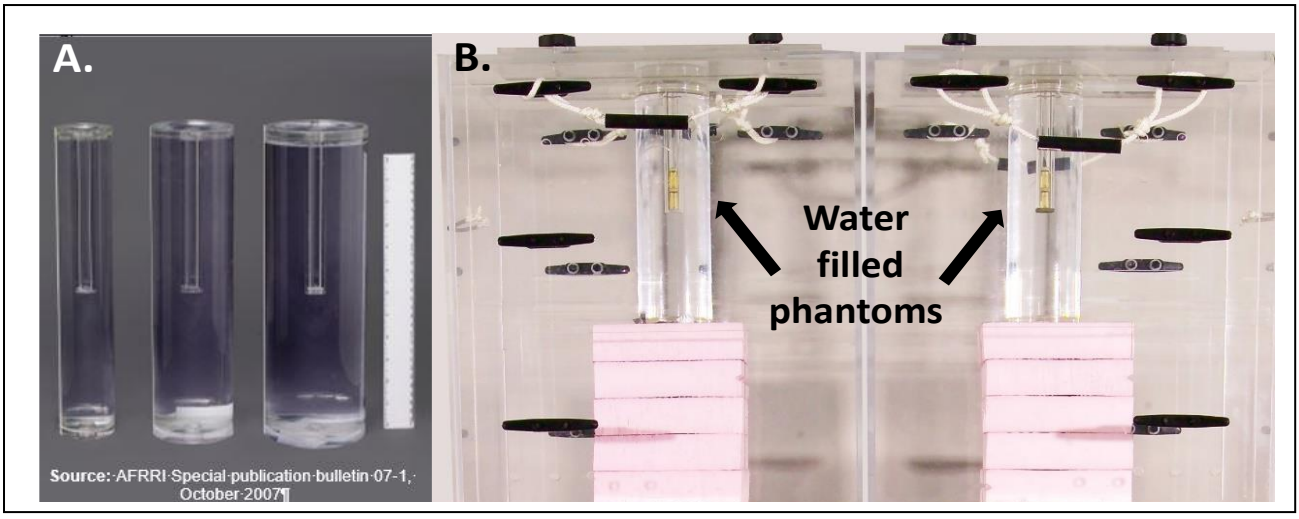

Fig. 2. Dose rate measurement using phantoms. (A) Cylindrical Plexiglas® phantoms of three different representative diameters (6.9, 10.0, and 12.5 cm) filled with water; the sleeves are for inserting polystyrene vials with alanine pellets into the cores of the phantoms. (B) Two Phantoms of identical diameters irradiated in the restraint boxes in the positions of the torsos of animals to be irradiated.

© 2025 European Society of Medicine

2.2. NON-HUMAN PRIMATE – RADIATION MODEL SYSTEM AND PERIPHERAL BLOOD BIOSAMPLING

The animal research was conducted according to the principles enunciated in the Guide for the Care and Use of Laboratory Animals (The Guide) prepared by the Institute of Laboratory Animal Resources, National Research Council, and were in full compliance with the recommendations for animal welfare and amelioration of suffering as recommended in the Weatherall Report on the use of non-human primates in research [26-27]. The study was approved by the AFRRI Institutional Animal Care and Use Committee (IACUC). Furthermore, this study, as are all those involving NHPs at AFRRI, received a 2nd tier review and approval by a designated independent DoD review agency for AFRRI's IACUC NHP protocols. AFRRI's Veterinary Sciences Department animal facility is accredited by the Association for Assessment and Accreditation of Laboratory Animal Care (AAALAC) International. The training of scientists and technicians for non-human primate (NHP) research activities were reviewed by AFRRI's IACUC. Male and female rhesus monkeys (*Macaca mulatta*) (~5.5 kg; ~4-yr old at the time of exposure; n = 28; two sham-treated animals were reused in a radiation cohort) were used in these studies. See Table 1 for additional dose-dependent details on gender, age at exposure, body weight and width for NHPs. These animals were obtained from a Department of Defense approved vender and were transported to the AFRRI Veterinary Sciences Department animal facility by an animal transporter certified for use of non-human primates and scheduled to minimize the transport period. Animals were housed in individual stainless-steel cages in conventional holding rooms at the AFRRI's Veterinary Sciences Department animal facility. Animal caging conditions, husbandry, and biosampling protocols were in full compliance with "The Guide". Animals were also provided varied forms of psychological and environmental enrichments including fruit, vegetable or additional supplements, and various cage enrichment devices as well as contact with staff personnel. Anesthetics were used to ameliorate any potential suffering or pain as described below. A clinical assessment tool, developed for use with Rhesus Macaques, was used to assess the severity of ARS to assure the humane treatment of animal [28]. Animals available after the experiment were transferred to another Department of Defense laboratory for use in another study.

Animals in each cohort (n = 6), received TBI to a midline tissue dose of 1.0, 3.5, 6.5, and 8.5 Gy ^{60}Co-γ rays at the dose rate of approximately 60 cGy m^{1}, with a cohort (n = 6) as a sham control. Ketamine anesthetized animals (Ketaset [10 mg kg-1, i.m.], Fort Dodge Laboratories; Fort Dodge, Indiana) were placed in a Plexiglas® restraint chair (to which they had been previously habituated), allowed to regain consciousness and were irradiated bi-laterally in a pair.

Table 1. Animal models for radiation biomarker studies

Dose group Gy	Dose rate Gy min-^{1}	Gender* M/F	Age (yr) at Exposure X±SD (Range)	Body Weight kg X±SD (Range)	Body Width cm X±SD (Range)
0.0	NA	2/4	4.5±0.5 (3.7-4.8)	5.4±0.6 (4.7-6.1)	11.9±1.3 (10.2-14.0)
1.0	0.55	4/2	4.2±0.7 (3.8-5.5)	5.5±0.9 (4.8-6.9)	11.1±1.3 (8.9-12.8)
3.5	0.56	4/2	4.5±0.9 (3.8-5.9)	5.5±1.0 (4.4-7.4)	11.4±1.0 (10.2-12.8)
6.5	0.55	4/2	4.6±0.6 (3.7-5.4)	5.8±1.1 (4.6-7.8)	12.4±2.4 (10.2-16.6)
8.5	0.54	4/2	4.1±0.5 (3.7-5.0)	5.2±0.8 (4.3-6.6)	10.0±1.0 (8.9-10.2)

*There are 6 animals per each dose cohort.

Prior to irradiation and then 6, 24, 48, 72 and 96 h after irradiation, peripheral blood (<1.5 x 10^{-3} l) was drawn from NHPs venipuncture using a heparin wetted needle (23G) and syringe while under either Ketamine anesthesia or by chairing without anesthesia. Drawn blood was collected into a serum separator tube (Cat. # 365967, Becton Dickinson and Company, Franklin Lakes, NJ) and potassium EDTA vacutainer tubes (Cat. # 365974, Becton Dickinson). Blood in EDTA tubes for white blood cell count measurements were analyzed within several hours after biosampling. Blood collected into serum separator tubes for amylase activity were centrifuged at 800 x g (4 °C) and stored at 4 °C prior to analysis <3 d.

2.3 PERIPHERAL BLOOD CELL COUNTS

Complete blood cell counts and differentials, determined using clinical hematology analyzers (Bayer Advia 120, Bayer, Tarrytown, NY) as previously described, were evaluated immediately prior to irradiation and on d 1, 2, and 3 after exposure [16-17]. Three replicate measurements were performed for each sample.

2.4. SERUM AMYLASE ACTIVITY

Amylase activities from serum samples, measured using a clinical blood chemistry analyzer (Bayer Vitros 250, Ortho Clinical Diagnostics, Rochester, NY) as previously described, were determined prior to irradiation and on d 1, 2, and 3 after exposure [16-17]. Three replicate measurements were determined for each sample.

2.5. MULTIVARIATE ALGORITHMS TO PREDICT RADIATION DOSE AND HEMATOPOIETIC-ACUTE RADIATION SYNDROME SEVERITY

Algorithms to predict radiation dose and hematopoietic acute-radiation-syndrome (H-ARS) severity were

© 2025 European Society of Medicine

developed. Biomarker data was obtained from a previous study involving 30 NHPs exposed to the following radiation doses: Sham 0 Gy (n = 6); 1.0 Gy (n = 6), 3.5 Gy (n = 6); 6.5 Gy (n = 6) and 8.5 Gy (n = 6) [28]. A data table was developed based on the radiation dose, H-ARS severity, and including measured hematology and biochemical biomarkers. Measurements for lymphocytes (1d, 2d, 3d), neutrophil-lymphocyte ratio (1d), and serum amylase (1d) were entered into a correlation matrix (MedCalc Statistical Software version 19.26 Ostend, Belgum). The correlation matrix consisted of individual columns for the blood cell and proteomic markers for the 1-3d time points. Additional columns "Radiation Dose (Gy)"and "H-ARS Severity" were added designated as the "Dependent" variables. The Dependent variables (i.e., radiation dose, H-ARS severity) were separately correlated with the five biomarkers and their different timepoints using the "Stepwise" best statistical fit option for creating multivariate models for estimating "Radiation Dose" and "H-ARS Severity".

2.6 DATA ANALYSIS

Statistical software (Sigma Plot 11, UCit Instructional and Research Computing, Software Distribution Office, 303B Zimmer, Cincinnati, OH, 45221-0088) was used for statistical data analysis. Values of $P < 0.05$ were considered statistically significant by Wilcoxon Signed Rank test. Values are expressed as means ± SEM. In the case of hematology results Graph Pad (Boston, MA) was used with paired-t test to compare baseline values with results at various timepoints.

Results

3.1 DOSE RATE AND DOSE

The dose rate in the core of the abdomen of the primate depends on the length of the path of the beam from the animal surface to the abdomen core because of differences in radiation attenuation and, to a lesser extent, in radiation scatter. The reported dose for individual animals in this study is determined based on the animal's "abdomen core" or mid-body dose, defined here as the half-width of the animal in the described irradiation source and exposure geometry setup. Therefore, at the same positions of the radiation sources, dose rates to the abdomen cores on the same day were somewhat different for animals of different widths, which required slightly different exposure times for the same dose to the abdomen cores.

The dose rates were measured in a series of preliminary experiments before the study using the alanine-electron paramagnetic resonance (EPR) dosimetry system[18-20]. In each of such experiments, two phantoms of identical diameters were irradiated in Plexiglas® boxes that were subsequently used for irradiation of the primates (Fig. 2B). The results from this study are shown in Figure 3 and illustrate the effect of phantom diameter on the measured dose rates. The positions of the phantoms corresponded to the positions of the torsos of the animals in the subsequent animal irradiations. Each phantom contained eight alanine dosimeters in two Plexiglas® vials, as shown in Figure 2B. In order to provide sufficiently high doses (approximately 200 Gy) desirable for highly accurate EPR measurements, the phantoms were irradiated for 6 hours exactly. The resulted doses to each of the 16 dosimeters in the two phantoms were measured by EPR. The spectrometer had been calibrated with a standard alanine calibration set purchased from the US National Institute of Standards of Technology (NIST), which made the results of the dose measurements directly traceable to U.S. national radiation standards. The accuracy of the spectrometer calibration had been additionally verified by an inter-comparison with the U.K. National Physical Laboratory (Teddington, Middlesex, UK). Appropriate precautions were taken to minimize, and correct for, effects that produce very small, but still measurable systematic errors in alanine dosimetry [23-25,29]. The measured doses and the exposure times were used to determine the dose rates to the core of the phantoms of the chosen diameter on the day of irradiation. Dose rates measured in this way for phantoms of different diameters on different days were normalized to the same date (May 9, 2008) and fitted with an empirically found suitable function (Fig. 3). The empirical fit made it possible to determine the dose rates in the middle of a hypothetical phantom of any intermediate diameter by interpolation. This dose rates was assumed to be in the core of the abdomen of a primate whose width at the height of the prescription dose ("core of the abdomen") corresponded to the phantom diameter. ^{60}Co decay correction made it possible to determine the dose rates on any desired day. As NIST standard alanine dosimeters were calibrated in terms of dose to water, a correction factor 0.9906 had to be applied to the dose rates thus obtained to get dose rates to soft tissue (this factor is the ratio of mass energy-absorption coefficients for soft tissue and water at the ^{60}Co energy) [30].

© 2025 European Society of Medicine

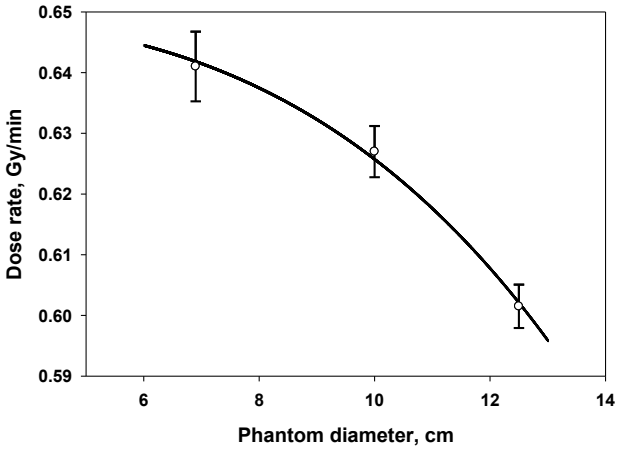

Fig. 3. Dose rate at the phantom core as a function of phantom diameter.

Dose rates determined in the way described above were used to calculate exposure times for animals of particular sizes on particular days of irradiations. The animals of similar mid-body widths were pair irradiated; their average mid-body widths were used to calculate the exposure time. Figure 4 illustrates some of the dose rate determinations. A contribution to the dose from irradiation while the sources were moving out of and into the pool (approximately 0.09 Gy) was measured separately with an ionization chamber. It was subtracted from the requested dose before its division by the calculated dose rate. The dose actually given to the animals were measured in real time with an ionization chamber. The dose rate used was 0.55 ± 0.004 (ranges from 0.54-0.56 Gy/min).

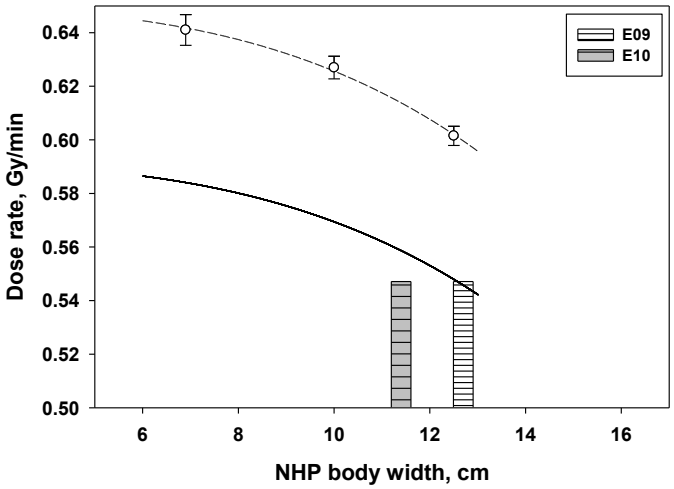

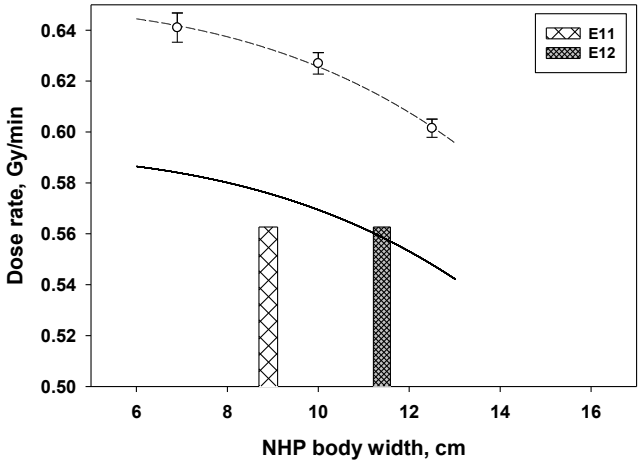

© 2025 European Society of Medicine

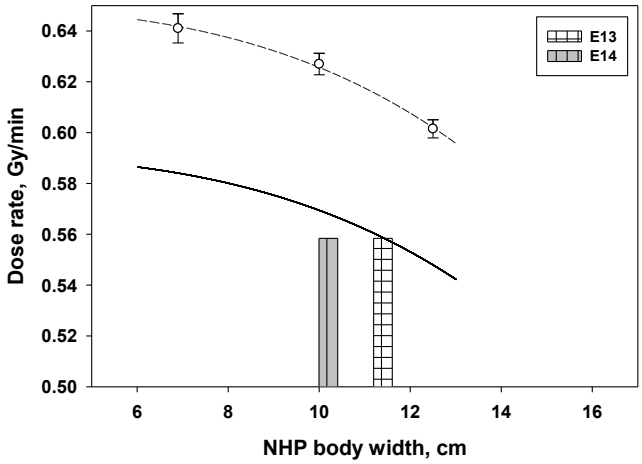

Fig. 4. Determinations of the dose rates for specific pairs of NHPs with varying lateral separations. The upper curve is an empirical least-squares fit of the dose rates measured in phantoms with alanine on the day of mapping. The lower curve shows dose rates on the day of the animal's irradiation (corrected for the ^{60}Co decay). The columns at the X axis show lateral body separations of the animals paired for each irradiation.

.

3.2 RADIATION FIELD UNIFORMITY

The uniformity of the radiation field was tested with radiographic films attached to foam blocks, which were positioned in the boxes at the locations of animals during the radiations (Fig. 5).

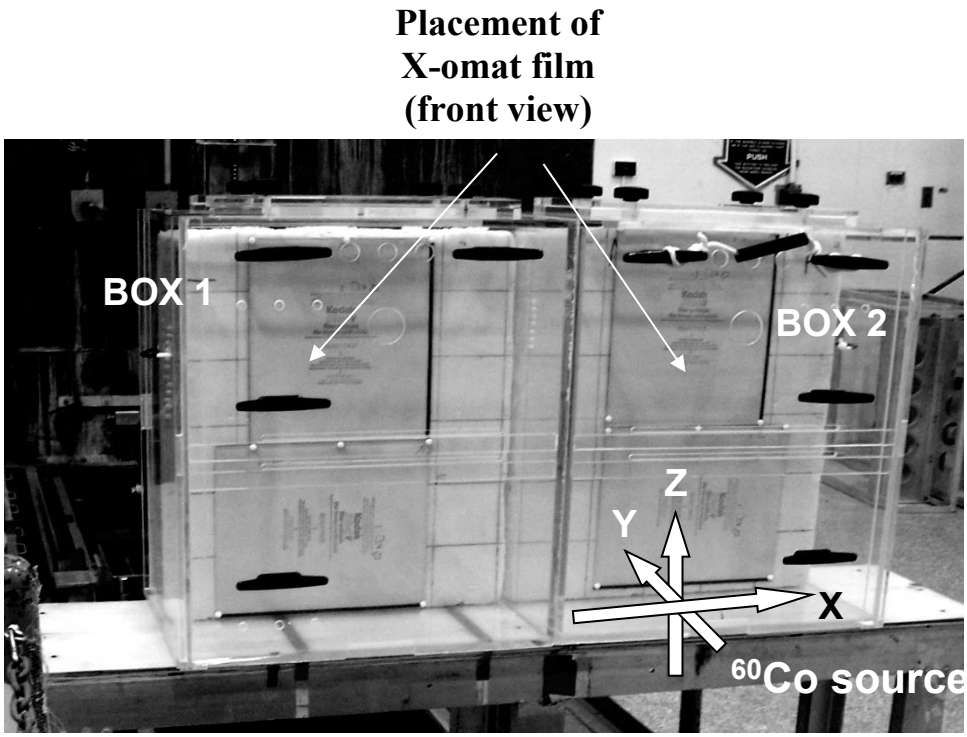

Fig. 5. Setup for measurements of the uniformity of the radiation field. Test of the field uniformity in the YZ plane (see Fig. 1 for coordinate designation). Tests of the field uniformity in the other planes are not shown here.

The data presented in Fig. 6 are for one of the boxes; the results for the other are very similar. The field in the area occupied by the animals was uniform within approximately ± 0.5% in the lateral direction, within approximately ± 1.5% in the anterior-posterior direction, and within approximately ± 2% along the superior-inferior direction. The slightly higher non-uniformity of the field in the vertical direction is due to the higher reflection of the beam from the pool water in the lower part and the non-uniform thickness of the walls of the boxes.

© 2025 European Society of Medicine

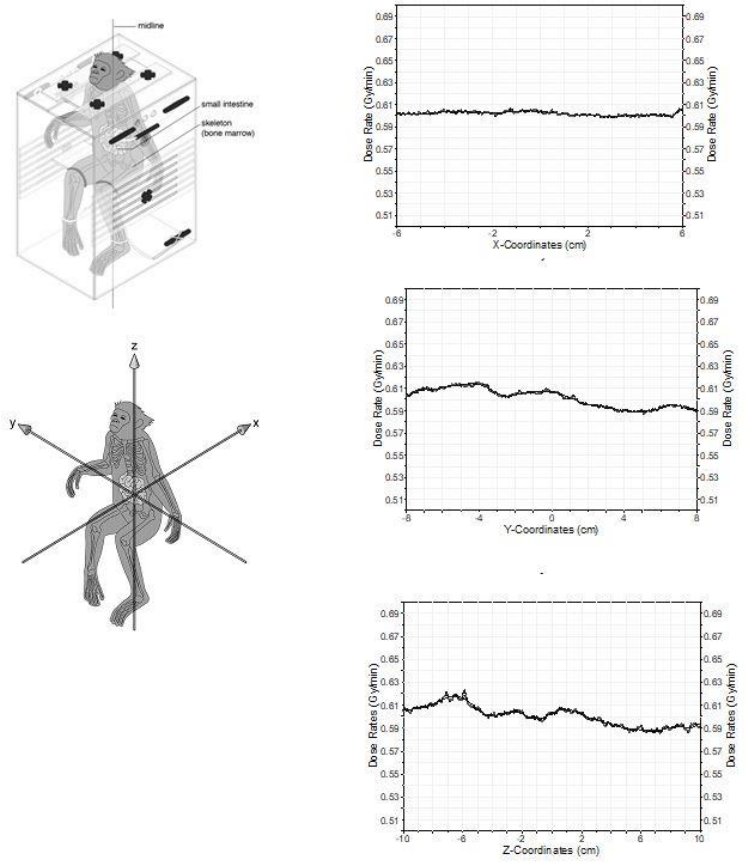

Fig. 6. Dose uniformity data obtained in experiment with exposure of Kodak V-Xomat radiographic films. Dose was measured for each of the coordinates (x, y, and z). Radiation coordinates are shown through the images of NHP in the restraint box.

3.3 AMYLASE ACTIVITY

Serum amylase activities in NHP's were measured prior as well as up to 4 d after irradiation. Mean baseline serum amylase activity was 372.1 (± 21.3) with values ranging from 251 to 718 UI^{-1}. Radiation-induced amylase activity at 24 h compared with controls was 1.3 (± .0.27; 1.0 to 1.9 -fold), 3.1 (± 1.43; 2.2 to 3.1 -fold)-, 9.4 (± 2.3; 2.0 to 8.3 -fold)- and 5.5 (± 2.6; 2.6 to 13.3 -fold) for NHP cohorts exposed to 1.0, 3.5, 6.5 and 8.5 Gy, respectively (Fig. 7). By 48 h after radiation the serum amylase activity value decreased relative to the peak values observed at 24 h (Fig. 7).

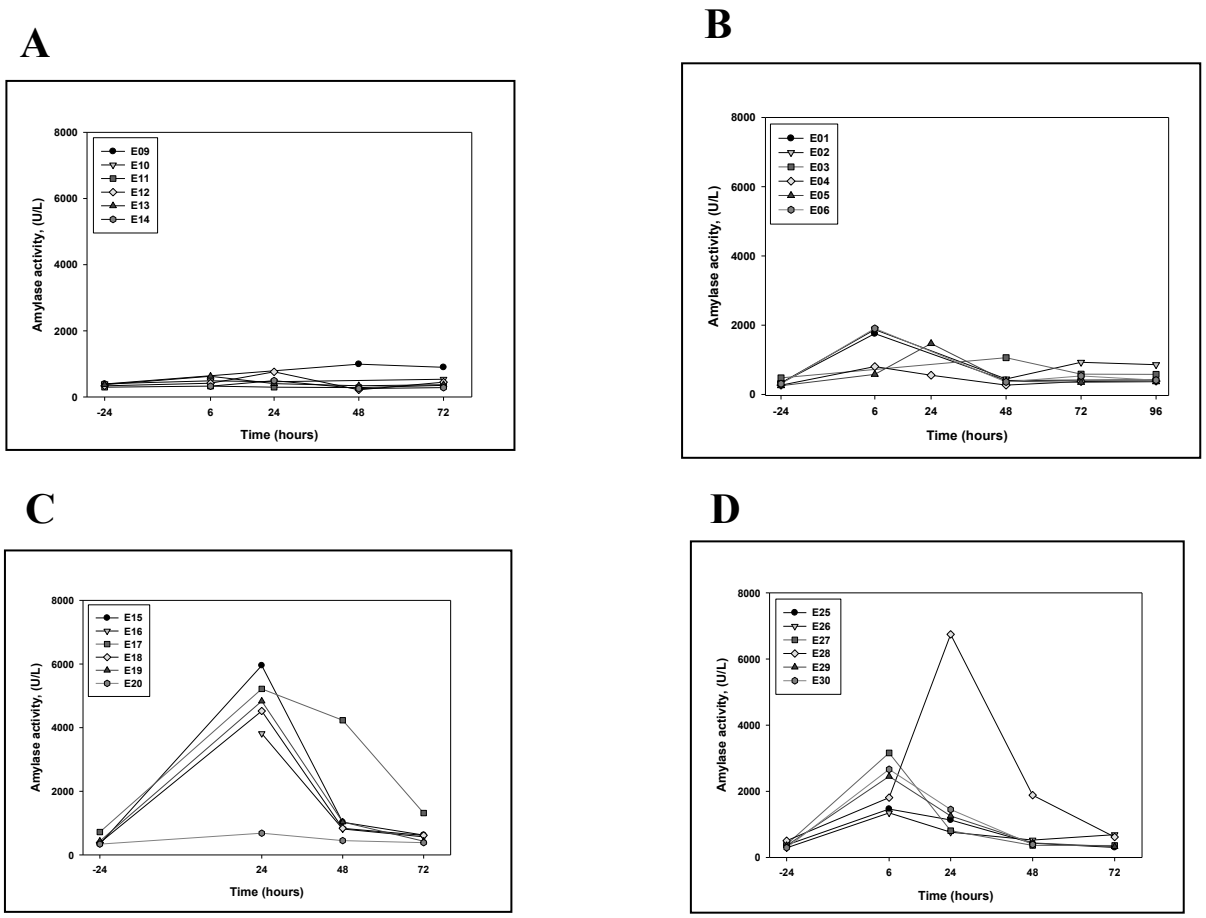

© 2025 European Society of Medicine

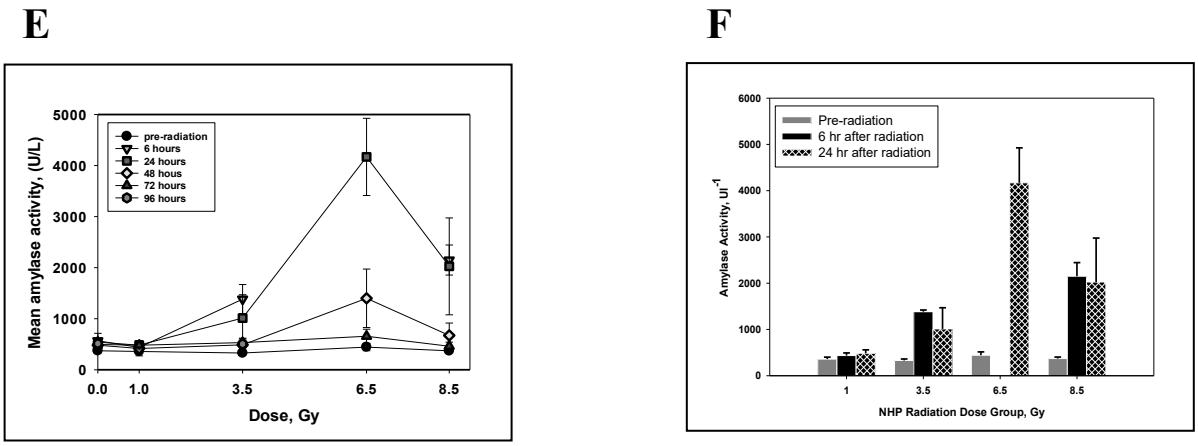

Fig. 7. Serum amylase activity in NHPs before and 4 d after irradiation. Activity profile of six animals exposed to (A) 1.0 Gy, (B) 3.5 Gy, (C) 6.5 Gy, and (D) 8.5 Gy. Mean serum amylase activity (E) with 0, 1, 3.5, 6.5, and 8.5 Gy exposure up to 4 d after irradiation. (F) Dose dependent relative increase of baseline serum amylase activity.

3.4 HEMATOLOGY

Blood cell counts for neutrophils and lymphocytes from each animal (under all radiation cohorts) were obtained before and at 6, 24, 48, 72 and 96 h after radiation exposure (Fig. 8, 9, & 10). Radiation causes a transient but not dose-dependent increase in neutrophil cell counts 6 h after irradiation for all four radiation doses (1.0, 3.5, 6.5 Gy and 8.5 Gy) relative to prior-radiation sampling (Fig 8 A, B, C, and D). At 1-d post exposure, the lymphocytes fall to 36 (± 8.5)%, 17 (± 4.3)%, 8 (± 1.7)% and 7 (± 0.95)% of baseline levels in the case of 1.0, 3.5, 6.5 and 8.5 Gy exposed animals, respectively (Fig. 9 A, B, C, and D).

© 2025 European Society of Medicine

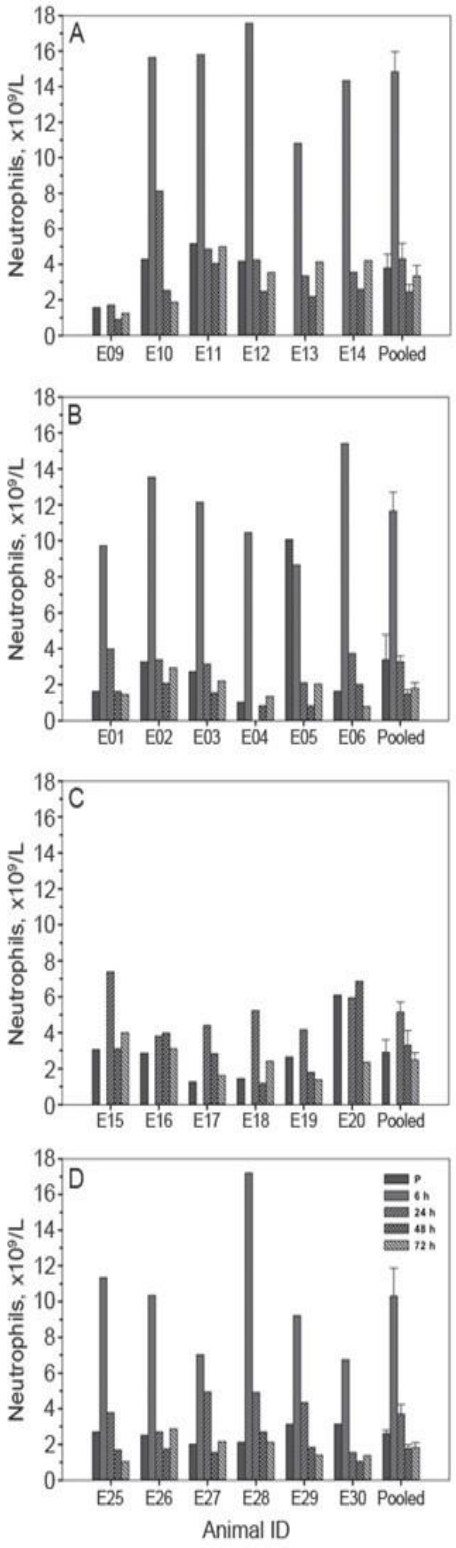

Fig. 8. Biological effects on neutrophil counts of NHPs (n = 6) after exposure to different doses of ^{60}Co-γ-rays. A, B, C, and D represents neutrophil counts from individual animals as well as from pooled animals, after 1.0 Gy, 3.5 Gy, 6.5 Gy, and 8.5 Gy radiation doses, respectively.

© 2025 European Society of Medicine

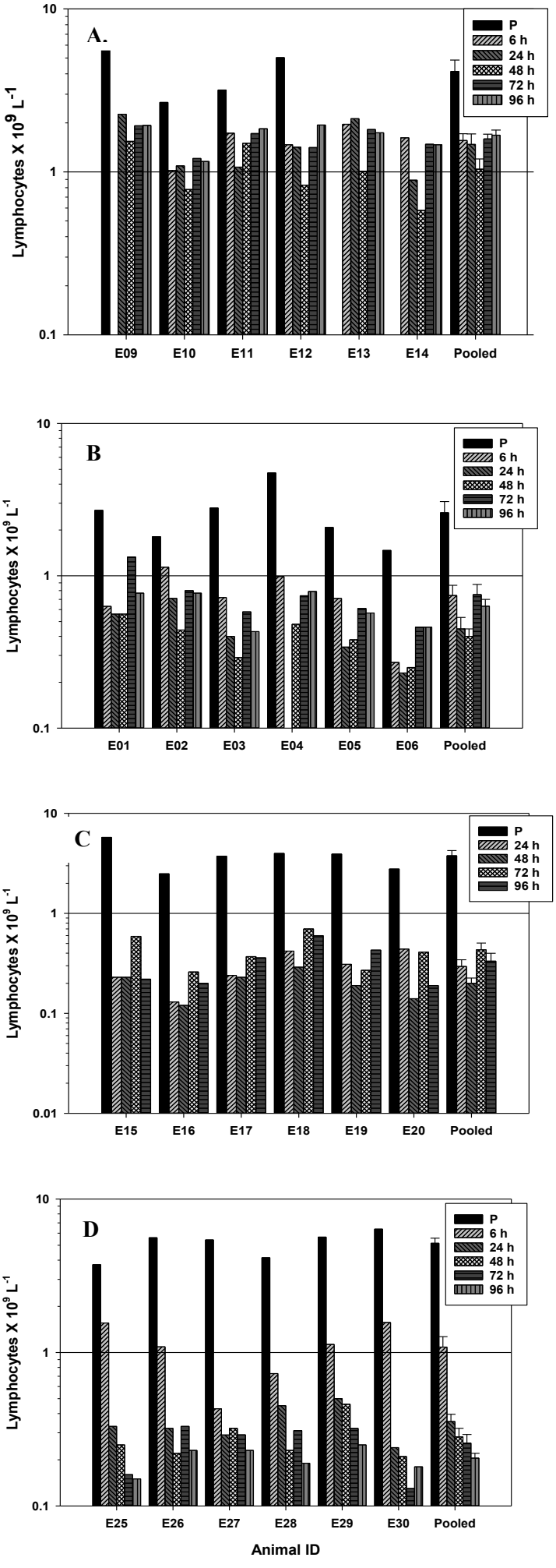

Fig. 9. Biological effects on lymphocyte counts of NHPs (n = 6) after exposure to different doses of ^{60}Co-γ-rays. A, B, C, and D represents lymphocyte counts from individual animals as well as from pooled animals, after 1.0 Gy, 3.5 Gy, 6.5 Gy, and 8.5 Gy radiation doses, respectively.

© 2025 European Society of Medicine

The baseline level of the ratio of neutrophils to lymphocytes ranged from 0.1413 to 4.8462 with a pooled cohort value of 0.7425 (SE ± 0.1145). Compared to baseline value, the ratio of neutrophils to lymphocytes elevated to 10.5 to 22-fold at 6 h for 1 and 8.5 Gy radiation doses ($P < 0.05$). At one day the comparison of the neutrophil to lymphocyte ratio values were significantly different from baseline ($P > 0.05$). After 1 d of irradiation the neutrophil to lymphocyte ratios were 3.7 (± 1.4), 5.3 (± 2.6), 22.7 (± 8.5) and 20.3 (± 3.6) fold for the four radiation doses, respectively (Fig 10 A, B, C, and D). The elevation of the ratio of neutrophils to lymphocytes compared with baselines persistent for 2 and 3 d for dose 1, 6.5, and 85 Gy ($P < 0.05$).

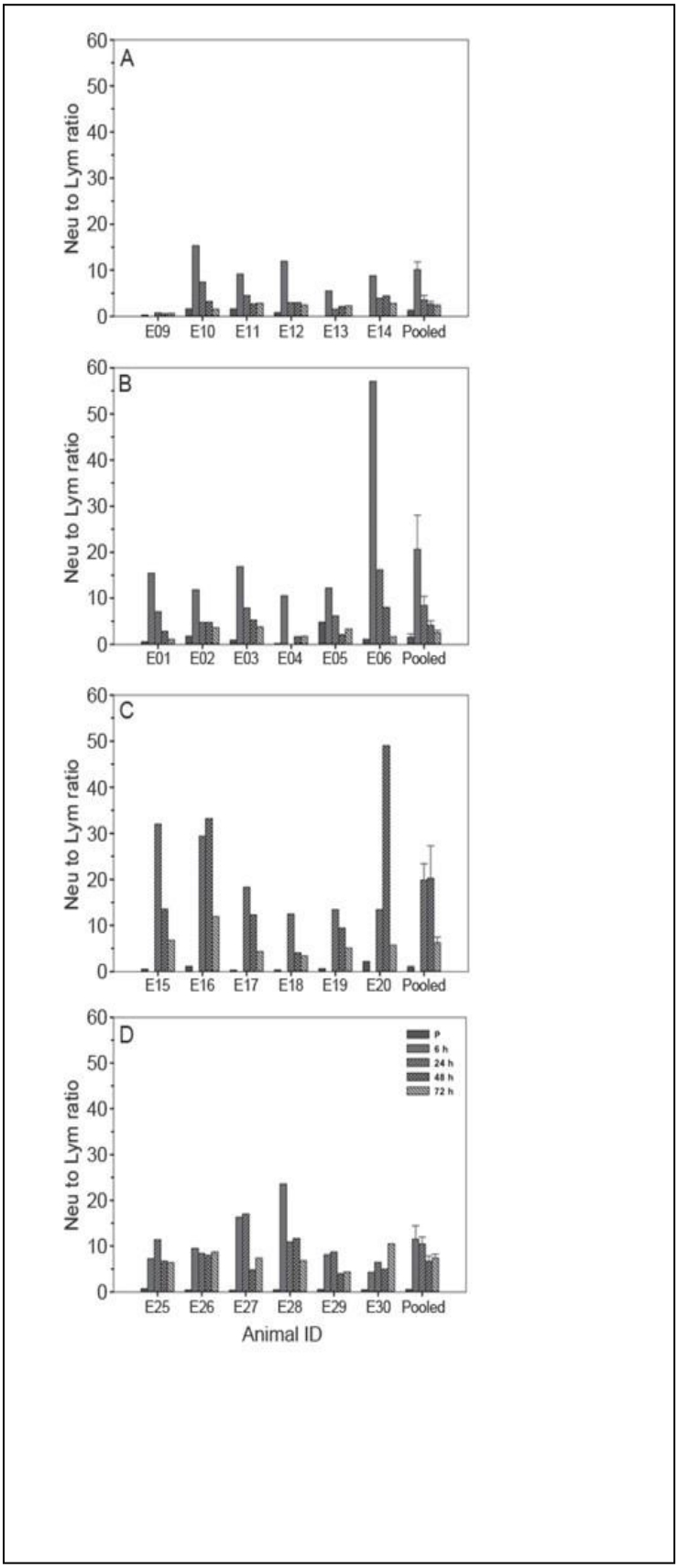

Fig. 10. Biological effects on neutrophil to lymphocyte ratio data of NHPs (n = 6) after exposure to different doses of ^{60}Co-γ-rays. A, B, C, and D represents neutrophil to lymphocyte ratios from individual animals as well as from pooled animals, after 1.0 Gy, 3.5 Gy, 6.5 Gy, and 8.5 Gy radiation doses, respectively.

© 2025 European Society of Medicine

3.5 EFFICACY OF MULTIVARIATE MODELING FOR "RADIATION DOSE" AND "*HEMATOPOIETIC-ACUTE RADIATION SYNDROM* " SEVERITY ESTIMATIONS

Multivariate modeling of radiation dose (Gy) using the variables amylase (1 d) and lymphocytes (3 d) with a sample size of 17, yielded an R-square value of 0.9149 with P-values of <0.0001 and 0.0034 respectively (Table 2). The F-ratio test (Larger Variance Estimate/Smaller variance Estimate), performed as part of the standard analysis by the MedCalc software, tested the significance of the independent variables used in the model. The F-ratio value (75.3011) was significant as was indicated by the P-value of <0.0001. From this value, it can be concluded that the R-squared result does not equal zero, and that the correlation between the model and dependent variable is statistically significant. The D'Agostino-Pearson test for Normal distribution indicated a P-value of 0.3237 accepting normality of the dataset used in the model.

Table 2. Multiple regression fit algorithms and statistical parameters for predicting radiation dose and hematopoietic acute radiation syndrome severity

Model		**Model 1**			**Model 2**	
Dose window, Gy		0 to 6.5			0 to 8.5	
Dependent variable		Dose, Gy			H-ARS severity, 0 to 4	
Sample size, n		17			22	
Coefficient of determination, R^2		0.9149			0.7591	
Regression equations						
Independent variables	Coefficient (Std. Error)	t	P	Coefficient (Std. Error)	t	P
(Constant)	1.5444			3.7181		
Amylase -1 d	0.00100 (0.0001228)	8.162	<0.0001			
Lymph – 2 d				0.6823 (0.2433)	2.805	0.0113
Lymph – 3 d	-0.3917 (0.1113)	-3.528	0.0034	-1.3106 (0.2796)	-4.687	0.0002
Analysis of variance						
Source	DF	Sum of Squares	Mean Squares	DF	Sum of Squares	Mean Squares
Regression	2	103.9002	51.9501	2	31.0891	15.5445
Residuals	14	9.6586	0.6899	19	9.8655	0.5192
F-ratio		75.3011	P<0.0001		29.9373	P<0.0001
D'Agostino-Pearson test for normal distribution		Accept Normality	P=0.3237		Accept Normality	P=0.6666

Multivariate modeling of H-ARS severity using the variables lymphocytes on 2 d and 3 d with a sample size of 22, yielded an R-square value of 0.7591 with P-values of <0.0113 and 0.0002 respectively (Table 2). The F-ratio value (29.9373) was significant as was indicated by the P-value of <0.0001. From this value, it can be concluded that the R-squared result does not equal zero, and that the correlation between the model and dependent variable is statistically significant. The D'Agostino-Pearson test for Normal distribution indicated a P-value of 0.6666 accepting normality of the dataset used in the model.

Discussion

Rhesus Macaques have been used in radiobiology studies as a research model for understanding human radio-responses using a variety of radiation qualities. For examples, NHPs have been exposed to electrons [31,32], x-rays,[31,33-34], γ-rays [35-37], protons [32,38-39], mixed proton energies [31], neutrons [40-41], and mixed neutron-γ-rays [42]. There can be significant dose exposure inhomogeneity in the irradiated NHPs in these investigations. Compared to whole-body irradiation of small animals such as mice, which are generally considered homogeneous for purposes of radiation dose estimations, irradiation of M. *mulatta*, especially large members of the species, presents challenges in providing accurate estimates of dose deposition to target tissues (i.e., alimentary canal, e.g., gut; and hematopoietic-cell-containing bones of the body, e.g., femur). Radiation studies reported as TBI using NHPs are likely to represent inhomogeneous radiation deposition in various target tissues. Factors contributing to difficulties in irradiating large animals include the (a) non-uniform distribution of radiosensitive tissues throughout the body, (b) non-uniform size of animals within treatment groups, and (c) physical location of radiosensitive proliferative tissues of the animal at the time of radiation exposure.

Reproducibility of NHP radiation exposures is critical to obtain meaningful results spanning a prolonged research study involving NHPs. Studies that have reported detailed radiation exposure and dosimetry characterizations for NHP irradiations are limited. In a

© 2025 European Society of Medicine

dosimetry study, NHPs were evaluated by using orthovoltage X ray (300 kV) and protons, [34] electrons and X-rays [31-32,38,] to obtain accurate information of the dose distribution. Zoetelief and colleagues performed dose measurements in homogeneous cylindrical phantoms of different sizes with 300kV X-rays for uni- and bilateral radiation to obtain more accurate information concerning the dose distribution in Rhesus monkeys, in particular with regard to the lung dose [34]. In a study evaluating pharmacokinetics and pharmacodynamics of ciprofloxacin (CIP) in irradiated NHPs, Nagy and colleagues characterized Alanine dosimetry and water filled cylindrical polymethyl methacrylate (PMMA) phantoms to accurately measure the dose distribution using 6.5 Gy cobalt-60 (^{60}Co) gamma photons [18]. Radiobiology studies have investigated both early- and late-phase effects.

Late-phase effects studies using NHP model systems have included investigations on TBI effects on skeletal growth, cataract development, chronic skin changes, incidence of tumors, etc. [33,40,43]. Doses greater than ≥7.50 Gy carry high risks for subsequent skeletal growth retardation and cataract development over a period of 5-10 y. Although whole-body exposure to ionizing radiation in rat and mouse results in incidence of late leukemia, both spontaneous and radiation induced leukemia are rare in the rhesus (Macaca mulatta) monkey. Single instance leukemia among a group of 36 animals exposed to fractionated low doses of whole-body neutron irradiation was reported after ten years of study [40]. Niemer-Tucker and colleagues evaluated Rhesus monkeys treated with TBI photon doses up to 8.5 Gy and proton doses up to 7.5 Gy at intervals up to 25-years post-radiation. Their results demonstrated no potential risk for eye-fundus pathology for doses up to 8.5 Gy. Cataract induction, however, was observed within 5 years after photon doses of 8.0 and 8.5 Gy and proton doses in excess of 2.5 Gy [39]. Kleef reported that only mild renal damage was evident after TBI of Rhesus monkeys with single doses of 4.5-8.5 Gy or two fractions of 5.4 Gy and even after follow-up times of 6-8 years [44].

Investigations of early-phase effects using TBI NHPs have included studies on physical activity, specific organ injuries, and the acute radiation syndromes. Using male rhesus monkeys Franz demonstrated that radiation causes transient (<2 h) incapacitation of physical activity (i.e., locomotor activity) [42]. Dose-dependent decreases in body weight, ponderal index, skinfold thickness, and thyroid weight were reported by Bakker and colleagues [45]. Stephens and colleagues studied radiation injury in rhesus salivary glands. Degeneration and necrosis of serous cells in both parotid and submandibular glands are clearly express by 24 h post irradiation and occur in a dose-related fashion [46]. Although parotid acinar cells are well-differentiated non-dividing cells, observations show that they express lethal radiation injury in interphase within hours of receiving a radiation dose as low as 2.5 Gy [47]. Late atrophy is the direct result of acute loss of serous acini and reflects a lack of regeneration of acinar cells receiving acute injury. Acute and chronic salivary gland dysfunctions are well known and a typical sequela of radiotherapy for head and neck cancer in humans. In order to study risks to man for the acute radiation syndrome, Dixon and Broerse et al., investigated TBI of Rhesus monkeys to doses resulting in both bone marrow and gastrointestinal sub-syndromes [41,48].

Animal models, including Rhesus monkeys, are also useful for studies addressing current protectors, mitigators, treatments, and biodosimetry. The NHP model provides an avenue for studies of multiple syndromes or late/delayed effects and is generally considered the most relevant animal model for human radio-response. Current research gaps exist in the evaluation and development of improved protectors, mitigators, and treatments. A meeting report described several needs: a) hematological data for irradiations other than high dose rate, low-LET radiation, b) identification and validation of new biomarkers for lethality and late effects (e.g. fibrosis, cancer), c) studies with partial-body exposure, co-morbidities, etc., and d) deployable diagnostic technologies for triage and treatment decisions [49]. The mechanisms through which radiation injury becomes manifest are not fully understood. Radiation injury responses varies from tissue to tissue and depends on the circumstances of the exposure, such as dose of radiation, protraction of exposure, and concomitant exposure to other noxious agents or tissue trauma. Research studies have focused on hematopoietic, gastrointestinal, central nervous system, kidney and lung towards the prophylaxis, mitigation and treatment of radiation injury [50].

Dubois and colleagues have demonstrated that intra-gastric administration of Zacopride (an antiemetic and gastro-kinetic agent) significantly inhibit radiation induced retching, vomiting, and suppression of gastric emptying in rhesus monkeys and did not cause detectable behavioral side effects when given to non-irradiated monkeys [51]. MacVittie and Farese using an NHP radiation model report that cytokine therapy promotes survival of genomically damaged hematopoietic stem cells (HSCs) by repairing sub-lethal damage to the genome and diminishing induction of the apoptotic pathway [52]. Use of a single therapeutic agent, AED (5-androstenediol), was found to be able to promote multilineage hematopoietic recovery of the bone marrow in the case of TBI of non-human primates [53]. Although a chemical inhibitor of the pro-apoptotic p53 pathway safeguarded animals from major lethal acute radiation syndrome, wild-type p53 plays an unexpected role as a survival factor in GI cells exposed to high doses of gamma irradiation, limiting the usefulness of p53 inhibitors as protection against hematopoietic (HP), but not GI acute radiation syndrome. Another promising therapeutic agent, CBLB502 - an agonist of TLR5 (Toll like receptor 5), was demonstrated in an NHP radiation model to afford protection against both bone marrow and GI acute radiation subsyndromes [54].

In an assessment analysis of three cytogenetic methods (dicentrics, micronuclei, and premature chromosome condensation), Darroudi and colleagues showed that blood count analysis was not suitable for discriminating between total body (TB) and partial body (PB) exposure. By using Poisson or overdispersion distribution as the basis, it was not possible to distinguish TB from PB irradiation when dicentric chromosomes and MN

(micronuclei) were analyzed. premature chromosome condensation (PCC) analysis, in contrast, showed a Poisson distribution after TBI and over dispersion after PBI. Using PCC assay, reliable dose estimates could be obtained up to 7 days after irradiation [55].

Potential for nuclear and radiological emergencies involving mass casualties from accidental or malicious acts is emerging from the worldwide situation. Current methodologies to rapidly assess radiation exposure and injury need to be enhanced to provide necessary diagnostic information to support early-phase medical treatment decisions [3]. Validation of candidate biodosimetric indices as part of radiological medical countermeasure studies, especially involving non-human primate radiation models, has significant merit to fill gaps in existing capabilities [26]. In this study as a part of an ongoing multiple parameter biodosimetry assay on non-human primate, we have tried to characterize the radiation exposure parameters and radio-response for early-phase hematology and blood chemistry biomarkers.

Blood biochemical markers of radiation exposure have been advocated for use in early triage of radiation casualties [16,56-58]. An increase in serum amylase activity (hyperamylasemia) from the irradiation of salivary tissue has been proposed as a biochemical measure of early radiation effect in a normal tissue [59-60] and as a candidate biochemical dosimeter in man [61-63]. These concepts are based on studies involving radio-iodine therapy [64-66], radiation therapy [60,62,67-68], and recently a radiation accident [63]. Although the epithelial cells of salivary gland divide rarely, in man, the salivary gland shows a high sensitivity to ionizing radiation. A few hours after irradiation injury, cells in the salivary gland show acute inflammation and degenerative changes resulting in increase in serum amylase activity.

Early after head and neck irradiation, serum amylase activity increases in human [69] and generally show peak values between 18-30 h after exposure, returning to normal levels within a few days [67]. Sigmoidal dose dependant increases in the early (1 d) hyperamylasemia are supported by radio-iodine therapy [65-66], radiotherapy [61-62,70], and limited data from three individuals exposed in a criticality accident [63]. In the dose response study, significant inter-individual variations are reported [60,67-68], which represent a major confounder for use of serum amylase activity alone as a reliable biodosimeter. Results [16] using rhesus monkeys are consistent with the observation of significant inter-individual variation (3.4-30.5 fold at 1 d after irradiation) following exposure to whole body acute radiation exposure (6.5 Gy ^{60}Co-γ rays). A similar pattern of results was found in our present study with amylase activity 1 d after the NHPs were exposed to 1.0, 3.5, 6.5, and 8.5 Gy (1.0 - 1.9 fold, 2.2 - 3.1 fold, 2.0 - 8.3 fold and 2.6 – 13.3 fold, respectively), with a pooled cohort value of 1.3 ± 0.27 fold, 3.1±1.43 fold, 9.4 ± 2.3 fold and 5.5 ± 2.6 fold, respectively. Baseline amylase activity increase (Fig. 7F) at different dose level exposures, specially at higher doses, increase of serum amylase activity at 24 h after 6.5 Gy radiation exposure (9.4 ± 2.3) and 8.5 Gy radiation exposure (5.5 ± 2.6) generally consistent with the levels predicted at these doses based on the human sigmoidal dose-response relationship reported earlier [68].

This group recommends a peripheral blood-serum amylase activity bioassay to provide an early indication of irradiation injury of the salivary glands and in combination with other biological parameters as a way to estimate severity of damage induced by accidental irradiation.

Hematological biomarkers of exposure to ionizing radiation are well characterized and used in medical management of radiological casualties [71]. Radiation causes a dose- and time-dependant depletion of lymphocytes [13,14]. Our findings show after 24 h the baseline levels of lymphocytes were depleted >60% with 1.0-Gy, >80% with 3.5-Gy, and >90% with 6.5- and 8.5-Gy radiation exposures, which were consistent with results drawn from irradiation accident registries [13]. We also observed time-dependent changes in neutrophil cell numbers after irradiation that are consistent with the consensus of early-phase radiation induced granulocyte cell count changes reported earlier [72-73]. Neutrophil to lymphocyte ratio (N/L) is a useful diagnostic indicator of severe radiation exposure [74]. Use of N/L ratios appears to normalize for inter-individual variations in lymphocyte and neutrophil cell concentrations, and potentially provides an enhanced signal to noise discrimination index of radiation exposure. Baseline N/L ratios from the pooled cohorts were 1.18±0.23 and increased to 3.3±1.4, 5.3±2.6, 22.7±8.5 and 20.3±3.5 in case of 1.0 Gy, 3.5 Gy, 6.5 Gy, and 8.5 Gy respectively, 24 h after exposure, supporting their diagnostic use in radiation exposure assessment.

Algorithms based on early-phase changes in biological markers for assessment of radiation dose and H-ARS severity were recently reviewed [10,75-76]. Potential biomarkers used for these purposes include blood cell count changes, biochemical assays (i.e., serum amylase, C-reactive protein, etc.), plasma proteomic biomarkers, and gene expression changes. In 2007 Goans and colleagues reported an algorithm for radiation dose prediction based on early lymphocyte depletion [13]. Port and Abend have developed a software tool (H-module) based on early-phase blood cell counts to predict H-ARS severity [77-78]. Ossetrova and colleagues used plasma proteomic biomarkers in a NHP radiation model to develop a radiation dose algorithm [19]. Sproull and colleagues using a murine radiation model reported on the use of organ-specific plasma proteomic biomarkers for radiation dose algorithms for total-body and partial-body exposures [79-80]. Bolduc, Blakely and colleagues have combined the use of proteomic and hematology biomarkers for prediction of H-ARS severity in a baboon, NHP, and minipig radiation models [81-82]. Port and Abend using the same baboon radiation model developed algorithms for prediction of H-ARS severity based on mRNA and miRNA expression changes [83]. Here we have used an NHP dose-response model and employed readily available early-phase blood cell count changes (i.e., lymphocytes) along with a biochemistry biomarker (i.e., serum amylase activity) to assess both radiation dose

and H-ARS severity. Use of algorithms for both radiation dose and injury can be complimentary for various aspects in the management of radiation incidents to include: i) initial triage in a radiation accident to develop early-phase medical management strategies and ii) retrospective reconstruction of the physical dose to characterize the radiation incident and long-term health consequences.

Conclusion

- Characterized exposure setup and radiation dosimetry including uniformity of dose, dose rate, and dose for use of an NHP radiation dose-response model;
- Reported on early-phase (<4 d) changes in hematology (i.e., lymphocytes, neutrophils, neutrophil to lymphocytes ratio) and biochemical (i.e., serum amylase activity) parameters;
- Developed algorithms to predict both radiation dose and H-ARS severity using NHP radiation model.

Conflict of Interest Statement:

None. The views expressed here are those of the authors; no endorsement by AFRRI has been given or inferred.

Acknowledgements:

The authors are grateful to Dr. Terry Pellmar, former Scientific Director of AFRRI for her willingness to transfer the grant and PI's responsibility to WFB. The authors gratefully acknowledge the assistance of Katya Krasnopolsky and Sergio Gallego in the processing of sample as well as experimental data and Katherine Cleveland for assistance in formatting the references. Authors also would like to acknowledge AFRRI Veterinarian Dr. Jennifer Mitchell for providing clinical advice and care for the NHPs, VSD technical care members SSG Anthony Klegenberg, SGT Benjamin Lowry, SGT Raymond McFadden, SGT Mark Gonzales, PFC Jessica Adams, Kevin Monfreda and Sarita Sherman for their tireless technical support in animal care and sample collections. We also wish to thank Sofia Echelmeyer (USUHS) for graphics support.

Funding Sources

Research was supported by DARPA's Radiation Biodosimetry Program – MIPR entitled: Non-human Primate Testing for Biodosimetry and under AFRRI project BD-13 (RBB4AR).

© 2025 European Society of Medicine

References

1. Dainiak N, Waselenko JK, Armitage JO, MacVittie TJ, Farese AM. The hematologist and radiation casualties. *Hematology Am Soc Hematol Educ Program*. 2003:473-96. doi:10.1182/asheducation-2003.1.473
2. Waselenko JK, MacVittie TJ, Blakely WF, et al. Medical management of the acute radiation syndrome: recommendations of the Strategic National Stockpile Radiation Working Group. *Ann Intern Med*. Jun 15 2004;140(12):1037-51. doi:10.7326/0003-4819-140-12-200406150-00015
3. Blakely WF, Salter CA, Prasanna PG. Early-response biological dosimetry--recommended countermeasure enhancements for mass-casualty radiological incidents and terrorism. *Health Phys*. Nov 2005;89(5):494-504. doi:10.1097/01.hp.0000175913.36594.a4
4. Goans RE, Waselenko JK. Medical management of radiological casualties. *Health Phys*. Nov 2005;89(5):505-12. doi:10.1097/01.hp.0000172144.94491.84
5. Swartz HM, Iwasaki A, Walczak T, et al. Measurements of clinically significant doses of ionizing radiation using non-invasive in vivo EPR spectroscopy of teeth in situ. *Appl Radiat Isot*. Feb 2005;62(2):293-9. doi:10.1016/j.apradiso.2004.08.016
6. National Council of Radiation Protection and Measurements. *Measurement of persons accidentally contaminated with radionuclides*. 1994. *NCPR Report No 65*. Available from: https://www.biblio.com/book/management-persons-accidentally-contaminated-radionuclides-recommendations/d/1045854443?srsltid=AfmBOoowq2iw28ZSA-lpZJ534sWt9rMJTb_GRMYeZmlqLbRNAyyjW0mm
7. National Council of Radiation Protection and Measurements. *Management of terrorist events involving radioactive material*. 2001. *NCPR Report No 138*. Available from: https://ncrponline.org/shop/reports/report-no-138-management-of-terrorist-events-involving-radioactive-material-2001/
8. National Council of Radiation Protection and Measurements. *Key elements of preparing emergency responders for nuclear and radiological terrorism*. 2005. *NCRP Commentary No 19*. Available from: https://ncrponline.org/shop/commentaries/commentary-no-19-key-elements-of-preparing-emergency-responders-for-nuclear-and-radiological-terrorism-2005/
9. Cohen KS. In: Gusev AE, Guskova AK, Mettler FA, Jr., eds. *Medical management of radiation accidents*. 2nd ed. CRC Press; 2001:chap Acute radiation sickness: underlying principles and assessment. Available from: https://www.taylorfrancis.com/chapters/mono/10.1201/9781420037197-10/acute-radiation-sickness-underlying-principles-assessment-kenneth-cohen-igor-gusev-angelina-guskova-fred-mettler
10. Blakely WF, Port M, Abend M. Early-response multiple-parameter biodosimetry and dosimetry: risk predictions. *J Radiol Prot*. Dec 6 2021;41(4)doi:10.1088/1361-6498/ac15df
11. Fliedner TM. Nuclear terrorism: the role of hematology in coping with its health consequences. *Curr Opin Hematol*. Nov 2006;13(6):436-44. doi:10.1097/01.moh.0000245696.77758.e6
12. Fliedner TM, Graessle D, Meineke V, Dorr H. Pathophysiological principles underlying the blood cell concentration responses used to assess the severity of effect after accidental whole-body radiation exposure: an essential basis for an evidence-based clinical triage. *Exp Hematol*. Apr 2007;35(4 Suppl 1):8-16. doi:10.1016/j.exphem.2007.01.006
13. Goans RE, Holloway EC, Berger ME, Ricks RC. Early dose assessment following severe radiation accidents. *Health Phys*. Apr 1997;72(4):513-8. doi:10.1097/00004032-199704000-00001
14. Goans RE, Holloway EC, Berger ME, Ricks RC. Early dose assessment in criticality accidents. *Health Phys*. Oct 2001;81(4):446-9. doi:10.1097/00004032-200110000-00009
15. Azizova TV, Osovets SV, Day RD, et al. Predictability of acute radiation injury severity. *Health Phys*. Mar 2008;94(3):255-63. doi:10.1097/01.HP.0000290833.66789.df
16. Blakely WF, Ossetrova NI, Mangalapus GL, et al. Amylase and blood cell-count hematological radiation-injury biomarkers in a rhesus monkey radiation model use of multiperameter and integrated biological dosimentry. *Radiation Measurements*. 2007;42(6-9):1164-1170. doi:10.1016/j.radmeas.2007.05.013
17. Blakely WF, Ossetrova NI, Whitnall MH, et al. Multiple parameter radiation injury assessment using a nonhuman primate radiation model-biodosimetry applications. *Health Phys*. Feb 2010;98(2):153-9. doi:10.1097/HP.0b013e3181b0306d
18. Nagy V, Parra NC, Shoemaker MO, Elliott TB, Ledney GD. Alanine dosimetry accurately determines radiation dose in nonhuman primates. *Armed Forces Radiobiology Research Institute Special Publication*. 2007:1-32.
19. Ossetrova NI, Blakely WF, Nagy V, et al. Non-human primate total-body irradiation model with limited and full medical supportive care including filgrastim for biodosimetry and injury assessment. *Radiat Prot Dosimetry*. Dec 2016;172(1-3):174-191. doi:10.1093/rpd/ncw176
20. Woods MJ, Collins SM. Half-life data-a critical review of TECDOC-619 update. *Appl Radiat Isot*. Feb-Apr 2004;60(2-4):257-62. doi:10.1016/j.apradiso.2003.11.026
21. International Standardization Organization and ASTM International. *ISO/ASTM 51607:2004*. Vol. 51607:2004(E). 2004. *Standard practice for use of an alanine-EPR dosimetry system*. Available from: https://www.iso.org/standard/39026.html
22. International Standardization Organization and ASTM International. *ISO/ASTM 51607:2013*. Vol. 51607:2013(E). 2013. *Standard practice for use of an alanine-EPR dosimetry system*. Available from: https://www.iso.org/standard/62955.html
23. Nagy V. Accuracy considerations in alanine dosimetry. *Appl Radiat Isot*. May 2000;52(5):1039-1050. doi:10.1016/S0969-8043(00)00052-X
24. Nagy V, Puhl JM, Desrosiers MF. Advancements in accuracy of the alanine dosimetry system. Part 2. The

© 2025 European Society of Medicine

influence of the irradiation temperature. *Radiat Phys Chem*. 2000;57(1):1-9. doi:10.1016/S0969-806X(99)00339-4
25. Nagy V, Sleptchonok OF, Desrosiers MF, Weber RT, Heiss AH. Advancements in accuracy of the alanine EPR dosimetry system. Part III: Usefulness of an adjacent reference sample. *Appl Radiat Isot*. 2000;59(4):429-441. doi:10.1016/S0969-806X(00)00275-9
26. National Research Council. *Guide for the care and use of laboratory animals*. 8th ed. National Academies Press; 2011.
27. Weatherall D, Working Group. *The use of non-human primates in research*. 2006:149. *A working group report chaired by Sir David Weatherall FMedSci*. 2006. Available from: https://acmedsci.ac.uk/file-download/34945-1165861003.pdf
28. King GL, Sandgren DJ, Mitchell JM, Bolduc DL, Blakely WF. System for scoring severity of acute radiation syndrome response in rhesus macaques (Macaca mulatta). *Comp Med*. Dec 1 2018;68(6):474-488. doi:10.30802/AALAS-CM-17-000106
29. Nagy V, Desrosiers MF. Complex time dependence of the EPR signal of irradiated L-α-alanine. *Appl Radiat Isot*. 1996;47(8):789-793. doi:10.1016/0969-8043(96)00053-X
30. Shleien B, Slaback LA, Jr., Birky BK. *Handbook of health physics and radiological health*. 3rd ed. Williams & Wilkins; 1998. Available from: https://books.google.com/books/about/Handbook_of_Health_Physics_and_Radiologi.html?id=j2vGQgAACAAJ
31. Fanton JW, Golden JG. Radiation-induced endometriosis in Macaca mulatta. *Radiat Res*. May 1991;126(2):141-6. doi:10.2307/3577812
32. Hardy KA. Dosimetry methods used in the studies of the effects of protons on primates: a review. *Radiat Res*. May 1991;126(2):120-6. doi:10.2307/3577809
33. Sonneveld P, van Bekkum DW. The effect of whole-body irradiation on skeletal growth in rhesus monkeys. *Radiology*. Mar 1979;130(3):789-91. doi:10.1148/130.3.789
34. Zoetelief J, Wagemaker G, Broerse JJ. Dosimetry for total body irradiation of rhesus monkeys with 300 kV X-rays. *Int J Radiat Biol*. Aug 1998;74(2):265-72. doi:10.1080/095530098141654
35. Mattsson JL, Yochmowitz MG. Radiation-induced emesis in monkeys. *Radiat Res*. Apr 1980;82(1):191-9. doi:10.2307/3575247
36. Cockerham LG, Forcino CD. Effect of antihistamines, disodium cromoglycate (DSCG) or methysergide on post-irradiation cerebral blood flow and mean systemic arterial blood pressure in primates after 25 Gy, whole-body, gamma irradiation. *J Radiat Res*. Jun 1995;36(2):77-90. doi:10.1269/jrr.36.77
37. Hao J, Sun L, Huang H, et al. Effects of recombinant human interleukin 11 on thrombocytopenia and neutropenia in irradiated rhesus monkeys. *Radiat Res*. Aug 2004;162(2):157-63. 15387143. doi:10.1667/rr3202
38. Wood DH. Long-term mortality and cancer risk in irradiated rhesus monkeys. *Radiat Res*. May 1991;126(2):132-40. doi:10.2307/3577811
39. Niemer-Tucker MM, Sterk CC, de Wolff-Rouendaal D, et al. Late ophthalmological complications after total body irradiation in non-human primates. *Int J Radiat Biol*. Apr 1999;75(4):465-72. doi:10.1080/095530099140393
40. Zalusky R, Ghidoni JJ, McKinley J, Leffingwell TP, Melville GS. Leukemia in the rhesus monkey (Macaca mulata) exposed to whole-body neutron irradiation. *Radiat Res*. Jun 1965;25:410-6. doi:10.2307/3571981
41. Broerse JJ, van Bekkum DW, Hollander CF, Davids JA. Mortality of monkeys after exposure to fission neutrons and the effect of autologous bone marrow transplantation. *Int J Radiat Biol Relat Stud Phys Chem Med*. Sep 1978;34(3):253-64. doi:10.1080/09553007814550841
42. Franz CG. Effects of mixed neutron-gamma total-body irradiation on physical activity performance of rhesus monkeys. *Radiat Res*. Mar 1985;101(3):434-41. doi:10.2307/3576502
43. Kirk JH, Casey HW, Traynor JE. Summary of latent effects in long term survivors of whole body irradiations in primates. *Life Sci Space Res*. 1972;10:165-73. doi:10.1515/9783112480144-022
44. van Kleef EM, Zurcher C, Oussoren YG, et al. Long-term effects of total-body irradiation on the kidney of rhesus monkeys. *Int J Radiat Biol*. May 2000;76(5):641-8. doi:10.1080/095530000138303
45. Bakker B, Massa GG, van Rijn AM, et al. Effects of total-body irradiation on growth, thyroid and pituitary gland in rhesus monkeys. *Radiother Oncol*. May 1999;51(2):187-92. doi:10.1016/s0167-8140(99)00059-6
46. Stephens LC, King GK, Peters LJ, Ang KK, Schultheiss TE, Jardine JH. Acute and late radiation injury in rhesus monkey parotid glands. Evidence of interphase cell death. *Am J Pathol*. Sep 1986;124(3):469-78. doi:10.1016/S0167-8140(86)80096-2
47. Stephens LC, Ang KK, Schultheiss TE, King GK, Brock WA, Peters LJ. Target cell and mode of radiation injury in rhesus salivary glands. *Radiother Oncol*. Oct 1986;7(2):165-74. doi:10.1016/s0167-8140(86)80096-2
48. Dixon B. The biological and clinical effects of acute whole or partial body irradiation. *J Soc Radiol Prot*. 1985;5(3):121-8. doi:10.1088/0260-2814/5/3/003
49. Augustine AD, Gondre-Lewis T, McBride W, Miller L, Pellmar TC, Rockwell S. Animal models for radiation injury, protection and therapy. *Radiat Res*. Jul 2005;164(1):100-9. doi:10.1667/rr3388
50. Stone HB, Moulder JE, Coleman CN, et al. Models for evaluating agents intended for the prophylaxix, mitigation and treatment of radiation injuries. Report of an NCI Workshop, December 3-4, 2003. *Radiat Res*. Dec 2004;162(6):711-728. doi:10.1667/rr3276
51. Dubois A, Nompleggi D, Castell DO. Histamine H2 receptor stimulation increases gastric emptying in monkeys. *Am J Physiol*. Dec 1988;255(6 Pt 1):G767-71. doi:10.1152/ajpgi.1988.255.6.G767
52. MacVittie TJ, Farese AM. Cytokine-based treatment of radiation injury: potential benefits after low-level

radiation exposure. *Mil Med*. Feb 2002;167(2 Suppl):68-70.
53. Stickney DR, Dowding C, Garsd A, et al. 5-androstenediol stimulates multilineage hematopoiesis in rhesus monkeys with radiation-induced myelosuppression. *Int Immunopharmacol*. Nov 2006;6(11):1706-13. doi:10.1016/j.intimp.2006.07.005
54. Burdelya LG, Krivokrysenko VI, Tallant TC, et al. An agonist of toll-like receptor 5 has radioprotective activity in mouse and primate models. *Science*. Apr 11 2008;320(5873):226-30. doi:10.1126/science.1154986
55. Darroudi F, Natarajan AT, Bentvelzen PA, et al. Detection of total- and partial-body irradiation in a monkey model: a comparative study of chromosomal aberration, micronucleus and premature chromosome condensation assays. *Int J Radiat Biol*. Aug 1998;74(2):207-15. doi:10.1080/095530098141582
56. Bertho JM, Demarquay C, Frick J, et al. Level of Flt3-ligand in plasma: a possible new bio-indicator for radiation-induced aplasia. *Int J Radiat Biol*. Jun 2001;77(6):703-12. doi:10.1080/09553000110043711
57. Blakely WF, Miller AC, Grace MB, et al. Radiation biodosimetry: applications for spaceflight. *Adv Space Res*. 2003;31(6):1487-93. doi:10.1016/s0273-1177(03)00085-1
58. Blakely WF, Miller AC, Grace MB, et al. Dose assessment based on molecular biomarkers. presented at: San Antionio, Texas Health Physics Society 36th Midyear Topical Meeting entitled "Radiation safety aspects of homeland security and emergency response" 2003; Alexandria, Virginia
59. Becciolini A, Giannardi G, Cionini L, Porciani S, Fallai C, Pirtoli L. Plasma amylase activity as a biochemical indicator of radiation injury to salivary glands. *Acta Radiol Oncol*. 1984;23(1):9-14. doi:10.3109/02841868409135978
60. Leslie MD, Dische S. Changes in serum and salivary amylase during radiotherapy for head and neck cancer: a comparison of conventionally fractionated radiotherapy with CHART. *Radiother Oncol*. May 1992;24(1):27-31. doi:10.1016/0167-8140(92)90350-4
61. Hofmann R, Schreiber GA, Willich N, Westhaus R, Bogl KW. Increased serum amylase in patients after radiotherapy as a probable bioindicator for radiation exposure. *Strahlenther Onkol*. Oct 1990;166(10):688-95.
62. Becciolini A, Porciani S, Lanini A, Balzi M, Faraoni P. Proposal for biochemical dosimeter for prolonged space flights. *Phys Med*. 2001;17 Suppl 1:185-6.
63. Akashi M, Hirama T, Tanosaki S, et al. Initial symptoms of acute radiation syndrome in the JCO criticality accident in Tokai-mura. *J Radiat Res*. Sep 2001;42 Suppl:S157-66. doi:10.1269/jrr.42.s157
64. Maier H, Bihl H. Effect of radioactive iodine therapy on parotid gland function. *Acta Otolaryngol*. Mar-Apr 1987;103(3-4):318-24. doi:10.3109/00016488709107290
65. Becciolini A, Porciani S, Lanini A, Benucci A, Castagnoli A, Pupi A. Serum amylase and tissue polypeptide antigen as biochemical indicator of salivary gland injury during iodine-131 therapy. *Eur J Nucl Med*. Oct 1994;21(10):1121-1125. doi:10.1007/bf00181068
66. Becciolini A, Porciani S, Lanini A. Marker determination for response monitoring: radiotherapy and disappearance curves. *Int J Biol Markers*. 1994;9(1):38-42. doi:10.1177/172460089400900108
67. Chen IW, Kereiakes JG, Silberstein EB, Aron BS, Saenger EL. Radiation-induced change in serum and urinary amylase levels in man. *Radiat Res*. Apr 1973;54(1):141-51. doi:10.2307/3573872
68. Dubray B, Girinski T, Thames HD, et al. Post-irradiation hyperamylasemia as a biological dosimeter. *Radiother Oncol*. May 1992;24(1):21-6. doi:10.1016/0167-8140(92)90349-y
69. Kashima HK, Kirkham WR, Andrews JR. Post-irradiation sialadenitis: a study of clinical features, histopathologic changes and serum enzyme variations following irradiation of human salivary glands. *Am J Roentgenol*. 1965;94:271-291.
70. Hennequin C, Cosset JM, Cailleux PE, et al. [Blood amylase: a biological marker in irradiation accidents? Preliminary results obtained at the Gustave-Roussy Institut (GRI) and a literature review]. *Bull Cancer*. 1989;76(6):617-24. L'amylasemie: un marqueur biologique des irradiations accidentelles? Resultats preliminaires obtenus a l'Institut Gustave-Roussy (IGR) et revue de la litterature.
71. Dainiak N. Hematologic consequences of exposure to ionizing radiation. *Exp Hematol*. Jun 2002;30(6):513-28. doi:10.1016/s0301-472x(02)00802-0
72. Fliedner TM, Friesecke L, Beyrer K. *Medical management of radiation accidents –manual on the acute radiation syndrome*. 2001. Available from: https://catalog.nlm.nih.gov/permalink/01NLM_INST/1o1phhn/alma9911303483406676
73. Graessle DH, Hofer EP, Lehn F, Fliedner TM. Classification of the individual medical severeness of radiation accidents within short time. presented at: The 10th Japanese-German Seminar, Nonlinear Problems in Dynamical Systems-Theory and applications; 2002; Noto Royal Hotel, Hakui, Ishikawa, Japan. Available from: https://scholar.google.com/scholar?q=Graessle+DH%2C+Hofer+EP%2C+Lehn+F%2C+Fliedner+TM.+Classification+of+the+individual+medical+severeness+of+radiation+accidents+within+short+time.+The+10th+Japanese-German+Seminar+on+Nonlinear+Problems+in+Dynamical+Systems%E2%80%94Theory+and+Applications%3B+September+30%E2%80%93October+3%2C+2002+at+the+Noto+Royal+Hotel%2C+Hakui%2C+Ishikawa%2C+Japan+%28unpublished+manuscript%29.
74. Zhang A, Azizova TV, Wald N, Day R. Changes of ratio of peripheral neutrophils and lymphocytes after radiation exposure may serve as a prognostic indicator of accident severity. presented at: Final program, 49th annual meeting of the Health Physics Society; 2004; McLean, Virginia.
75. Abend M, Blakely WF, Ostheim P, Schuele S, Port M. Early molecular markers for retrospective biodosimetry and prediction of acute health effects. *J*

© 2025 European Society of Medicine

Radiol Prot. Jan 25 2022;42(1)(42) doi:10.1088/1361-6498/ac2434

76. Blakely WF, Port M, Ostheim P, Abend M. Radiation Research Society journal-based historical review of the use of biomarkers for radiation dose and injury assessment: acute health effects predictions. *Radiat Res*. Aug 1 2024;202(2):185-204. doi:10.1667/RADE-24-00121.1
77. Port M, Abend M. Clinical triage of radiation casualties-the hematological module of the Bundeswehr Institute of Radiobiology. *Radiat Prot Dosimetry*. Dec 1 2018;182(1):90-92. doi:10.1093/rpd/ncy141
78. Port M, Haupt J, Ostheim P, et al. Software tools for the evaluation of clinical signs and symptoms in the medical management of acute radiation syndrome-a five-year experience. *Health Phys*. Apr 1 2021;120(4):400-409. doi:10.1097/HP.0000000000001353
79. Sproull M, Kawai T, Krauze A, Shankavaram U, Camphausen K. Prediction of total-body and partial-body exposures to radiation using plasma proteomic expression profiles. *Radiat Res*. Dec 1 2022;198(6):573-581. doi:10.1667/RADE-22-00074.1
80. Sproull M, Fan Y, Chen Q, Meerzaman D, Camphausen K. Organ-specific biodosimetry modeling using proteomic biomarkers of radiation exposure. *Radiat Res*. Oct 1 2024;202(4):697-705. doi:10.1667/RADE-24-00092.1
81. Bolduc DL, Bunger R, Moroni M, Blakely WF. Modeling H-ARS using hematological parameters: a comparison between the non-human primate and minipig. *Radiat Prot Dosimetry*. Dec 2016;172(1-3):161-173. doi:10.1093/rpd/ncw159
82. Blakely WF, Bolduc DL, Debad J, et al. Use of proteomic and hematology biomarkers for prediction of hematopoietic acute radiation syndrome severity in baboon radiation models. *Health Phys*. Jul 2018;115(1):29-36. doi:10.1097/HP.0000000000000819
83. Port M, Herodin F, Drouet M, et al. Gene expression changes in irradiated baboons: a summary and interpretation of a decade of findings. *Radiat Res*. Jun 1 2021;195(6):501-521. doi:10.1667/RADE-20-00217.1

© 2025 European Society of Medicine